Institute of Physics Publishing Journal of Physics D: Applied Physics
J. Phys. D: Appl. Phys. **36** (2003) 1009–1017 PII: S0022-3727(03)55788-6

Noise characteristics of resistors buried in low-temperature co-fired ceramics

A Kolek[1], **P Ptak**[1] **and A Dziedzic**[2]

[1] Department of Electronics Fundamentals, Rzeszów University of Technology, Wincentego Pola 2, Rzeszow, 35-959, Poland
[2] Faculty of Microsystem Electronics and Photonics, Wrocław University of Technology, Wybrzeże Wyspiańskiego 27, Wrocław, 50-370, Poland

E-mail: akoleknd@prz.rzeszow.pl and adziedzic@pwr.wroc.pl

Received 8 October 2002, in final form 31 January 2003
Published 2 April 2003
Online at stacks.iop.org/JPhysD/36/1009

Abstract
The comparison of noise properties of conventional thick film resistors prepared on alumina substrates and resistors embedded in low-temperature co-fired ceramics (LTCCs) is presented. Both types of resistors were prepared from commercially available resistive inks. Noise measurements of LTCC resistors below 1 kHz show Gaussian $1/f$ noise. This is concluded from the calculations of the second spectra as well as from studying the volume dependence of noise intensity. It has occurred that noise index of LTCC resistors on average is not worse than that of conventional resistors. A detailed study of co-fired surface resistors and co-fired buried resistors show that burying a resistor within LTCC substrate usually leads to (significant) enhancement of resistance but not of noise intensity. We interpret this behaviour as another argument in favour of tunnelling as the dominant conduction mechanism in LTCC resistors.

1. Introduction

The conductive oxide-based thick-film resistors are metal–insulator granular composites. These resistors are prepared by screen-printing of a suitable resistive ink onto a ceramic substrate. The ink is composed of nanometre or submicrometre sized grains of conductive oxide (e.g. RuO_2, IrO_2, $Bi_2Ru_2O_7$, $Pb_2Ru_2O_{7-x}$) mixed together with a glass frit and organic solvent. After printing onto a ceramic substrate the resistor is dried and fired at approximately 850˚C. Recently the development of low-temperature co-fired ceramic (LTCC) technology has enabled embedding (burying) passive components (resistors, capacitors, inductors) within a ceramic substrate in a single firing step. The low-temperature ceramic tapes are similar with respect to their solids content to most screen-printed low-permittivity thick-film dielectrics. But the organic resins and binders are changed to permit the slurry to be cast and dried into tape. These tapes typically consist of glass compounds mixed with alumina or silica. They possess the properties of both ceramics and glasses. One of the standard applications of LTCC technology is electronic package. LTCC substrates offer hermetic and reliable packaging with the possibility to have multiple layers and high-density internal interconnections. Of large importance occurring during co-firing of passive components and ceramic tape are physical and chemical compatibilities between different materials involved in such process [1–5]. The first example is the differential shrinkage and mismatch of thermal expansion coefficients of buried (resistive) material and dielectric surround, another one is the possibility of chemical reactions between these two materials. All these issues are systematically studied and the progress in understanding the relation between microstructure and electrical properties of buried resistors is continuously being made [6]. The experimental and theoretical approaches are mostly concerned with resistivity and its temperature dependence [6], the behaviour of the resistors at high-frequencies [7–9] and under DC voltages [7, 10] or high-voltage pulses [4]. Only very few papers deal with noise properties of resistors buried in the LTCCs. This paper summarizes our recent low-frequency noise measurements [8, 10, 11] and provides new arguments for the explanation of conduction mechanism and noise sources in LTCC resistors.

The aim of this paper is at least twofold. The first is to perform the extensive study of low-frequency noise properties of LTCC resistors. The question we shall answer is whether

 © 2003 IOP Publishing Ltd Printed in the UK

(and how) the ceramic substrate and the process of co-firing influence the noise index of the resistor. The second aim is to identify the sources of the noise in this kind of resistors. The main conclusion is that noise properties of LTCC resistors are not worse than those of conventional thick-film resistors on alumina substrates. Our results also show that burying a resistor in a LTCC substrate usually leads to (significant) increase of sheet resistance while the noise intensity is kept on the same level. We interpret this behaviour as a fingerprint of tunnelling conduction mechanism.

2. Sample preparation

Most of the resistors were screen-printed on alumina substrates or on Du Pont DP951 green tape. Some of them were printed on Ferro A6-M or Hereaus CT700 tapes. The test pattern usually consisted of 'small' square-shaped sample of dimensions: $0.3 \times 0.3\,\text{mm}^2$ (R4) and 'large' sample of dimensions $1.5 \times 1.5\,\text{mm}^2$ (R1). Sometimes the dimensions were $1 \times 1\,\text{mm}^2$ (R2) or $1.2 \times 1.2\,\text{mm}^2$ (R3) or $9 \times 1\,\text{mm}^2$ (R5). Altogether, three LTCC and one 'on alumina' structures were tested.

- Resistor on alumina substrate (A).
- Post-fired surface resistor (SP). Resistor is printed onto LTCC substrate which was previously laminated and fired in the first firing cycle. The resistor is fired in the second firing cycle.
- Co-fired surface resistor (SC). Resistor is printed onto a ceramic tape. The whole structure is then laminated and fired in the single process.
- Co-fired resistor buried in LTCC (B). Resistor is printed onto a ceramic tape and covered by another ceramic tape. The whole structure is then laminated and fired in the single process.

Most of the resistors were screen-printed through 400 mesh screen. Only very few resistors on alumina substrates were printed through 200 mesh screen. Commercially available DP2051 (100 kΩ per square), DP2041, DP8039, CF041 (10 kΩ per square) and CF021 (100 Ω per square) inks were used as a resistive material. Tab terminals were made from PdAg inks. The resistors were fired at 875˚C peak temperature during 60 min (SP and 'on alumina' processes) or 120 min (SC and B processes) firing cycles with 10 and 15 min soaking times, respectively. The sheet resistances of the specimens used in the experiments are gathered in table 1. These resistances were calculated from the slopes of current–voltage characteristics which occurred to be linear up to the highest voltages employed in the experiments (low- and high-field resistances never differed by more than 1%). Other properties of these resistors are discussed in [4, 8, 10, 12]. Most of the resistor series show normal dimensional effect, i.e. sheet resistance increases as resistor length increases. The exceptions from this rule are L2041B, L041B, L021B and all but one DP2051 series for which we observe abnormal dimensional effect (sheet resistance decreases when resistor length increases). The interesting connection that can be observed for DP8039 and DP2041 series is that resistance decreases when the 'strength' of the LTCC neighbourhood increases. The largest is the sheet resistance of A samples. It drops a little for SP samples and it further drops down for SC samples. The conjecture 'the more ceramic neighbourhood the lower resistance' would hold if it held for B samples. Unfortunately, it breaks down: when a resistor is buried, a large increase of the sheet resistance takes place. This experimental fact, which is observed also for DP2051, CF041 and CF021 series, emerges as a rule and suggests that something important happens when burying a resistor.

3. Experimental techniques

Noise measurements were carried out mostly by DC technique. The sample of resistance R was biased through the ballast, wire-wound resistor $R_B \gg R$ from DC voltage source. The noise signal was AC-coupled to the low-noise preamplifier Unipan 233-7 (bandwidth 0.5 Hz–100 kHz) and then sent to HP 35660A signal analyser for Fourier transforming. More than 250 FFTs were taken to obtain power spectral density S_V. The latter was measured in the frequency range 2–800 Hz for several voltages V biasing the sample (see figure 1). After

Table 1. Sheet resistances (in Ω per square) of all specimens used in the experiment.

Paste	Substrate	Description	R1	R2	R3	R4	R5
DP8039	Al_2O_3	A8039/200	16 258	—	—	10 155	—
DP8039	Al_2O_3	A8039/400	32 855	—	—	13 460	—
DP8039	DP951	L8039SP	8 890	—	—	7608	—
DP8039	DP951	L8039SC	5 830	—	—	3409	—
DP8039	DP951	L8039B	27 411	—	—	8890	—
DP2041	Al_2O_3	A2041/200	11 249	—	—	3418	—
DP2041	DP951	L2041SP	12 411	—	—	6075	—
DP2041	DP951	L2041SC	6 869	—	—	4151	—
DP2041	DP951	L2041B	34 943	—	—	63 435	—
DP2051	DP951	L2051SC	—	93 481	—	—	71 887
DP2051	DP951	L2051B	—	133 290	—	—	120 440
DP2051	A6-M	L2051SC(F)	—	55 579	—	—	74 164
DP2051	A6-M	L2051B(F)	—	63 368	—	—	41 564
DP2051	CT700	L2051B(H)	—	123 480	—	—	92 200
CF041	DP951	L041SC	—	—	2988	2200	—
CF041	DP951	L041B	—	—	10 716	12 448	—
CF021	DP951	L021SC	—	—	38.8	37.6	—
CF021	DP951	L021B	—	—	98	208	—

subtracting the noise background $S_{V=0}$, which is the sum of preamplifier noise and thermal noise, it has occurred that the spectra have $1/f$ shape (see figure 2(*a*)). So, we use the average $\langle f S_V \rangle$ over the frequency band 2–800 Hz to estimate a frequency independent noise level. It is still bias dependent. When $\log\langle f S_V \rangle$ is displayed versus $\log V$ the lines drawn through the data have the slope of approximately 2. This means that relation $S_V \sim V^2$ holds and the physical origin of the noise are equilibrium resistance fluctuations. The successive steps of this procedure are illustrated in figure 2.

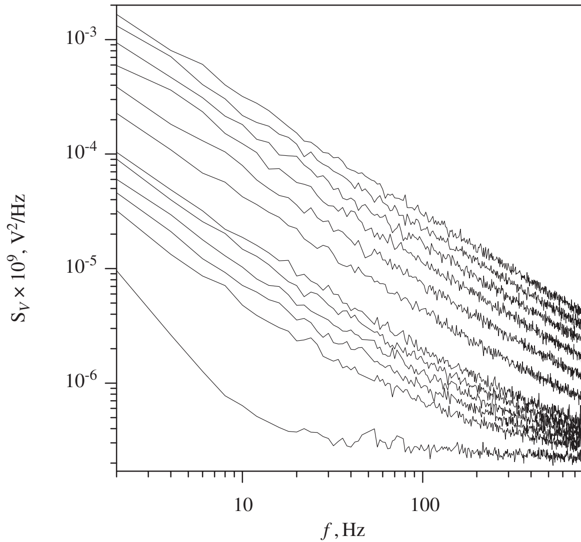

Figure 1. Power spectral densities S_V of voltage fluctuation 'as-measured' for L2041SP resistor R1. Successive lines from the bottom to the top are for increasing bias voltage V. The lowest curve is for $V = 0$ (background noise). Successive spectra are for $V = 2.4$, 3.0, 3.6, 4.2, 4.8, 7.6, 10.2, 12.8, 15.3, 17.9 and 20.4 V.

In case of the low-resistance series CF021 (and also for medium resistance series CF041) noise measurements were performed by the AC technique, which is known to be more sensitive and allows detection of noise signal at much lower excitation [13]. The measurement set-up for this technique is shown in figure 3. A sample of resistance R was placed in one of the bottom arms of the Wheatstone bridge and excited through the ballast resistor $R_B \gg R$ by AC current $I = I_0 \cos(2\pi f_0 t)$. Adjustable resistor R_{B1} in the opposite arm of the bridge was used to balance the bridge. The signal was taken from the bridge diagonal. It was then amplified, multiplied by $\cos(2\pi f_0 t)$ in a phase-sensitive detector, low-pass filtered to reject '$2f_0$' component and eventually Fourier transformed. The main advantage of AC method is that excess noise at the frequency f, is masked by the background noise not at the same frequency f, but rather at frequencies $f_0 \pm f$. At these frequencies the major component of the background noise is thermal noise whereas preamplifier's noise is quite low. For $f \to 0$ the background noise spectrum ($\cong S_{V=0}(f_0)$) is flat down to 0 Hz. In contrast, excess noise has usually $1/f$ spectrum, and in mHz frequencies exceeds the background even for low bias. As a result much lower voltages are required to make the measurements.

The excitation frequency used in our measurements was $f_0 = 325$ Hz. This value was chosen in order to make the signals arising from mixing f_0 and higher order harmonics of line frequency (50 Hz) as low as possible and to make differential frequencies as high as possible. We observed that 300 and 350 Hz harmonics had the lowest amplitudes and so f_0 was set in the middle of this range. In the spectrum of the input signal the peaks arising from mixing frequencies 300 and 350 Hz with f_0 appear than at 25 Hz. Below this value the spectrum is free from any disrupting peaks. Power spectral densities were gathered in a frequency range of 62.5 mHz–3 Hz

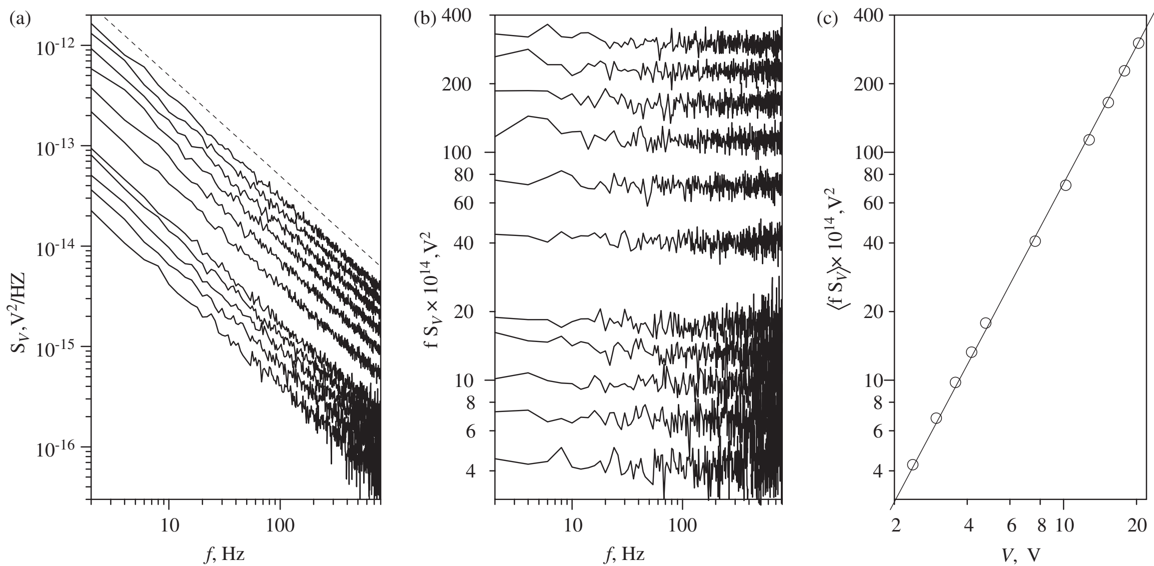

Figure 2. (*a*) Power spectral densities S_V of 'excess' noise obtained from those in figure 1 by subtracting noise background, $S_{V=0}$. Dashed line shows pure $1/f$ spectrum. (*b*) The product of frequency and power spectral density calculated for the data from (*a*). Curves are almost frequency independent, and so in (*c*) the product $f S_V$ averaged over the bandwidth 2–800 Hz ($\langle\ \rangle$) is plotted versus the voltage V biasing the sample. The approximating line is the graph of the function $\langle f S_V \rangle = 7.3 \times 10^{-15}$ V^2. Voltage independent noise index $S \equiv \langle f S_V \rangle / V^2 = 7.3 \times 10^{-15}$.

with a resolution of 62.5 mHz. For such resolution single time record lasts 16 s, and so subsequent time records were allowed to overlap each other. On the one hand, this makes the spectra more 'rough' as one can see in figure 4(*a*), but on the other hand, this makes the overall time of collecting data much smaller and prevents components due to long time drifts appearing in the spectra [14]. The spectra were measured for several rms voltages applied to the sample (see figure 4). Further steps of the procedure were as in DC case. The only difference is that now the product fS_V is averaged over the band 62.5 mHz–3 Hz. Data in figure 4 show that with AC method a reasonable detection of noise signal is possible at the voltage as low as 0.1 V_{rms}. This is much lower than voltages applied in DC technique (compare with figure 2(*a*)). For this reason the AC method is very useful for the low-resistance, low-noise samples for which the use of large bias would lead to the self-heating and non-linear effects.

For low-resistance series CF021 the noise level was so low that the recognition of $1/f$ shape of the spectra was difficult. So, we use the difference $S_V - S_{V=0}$ integrated over the band 0.1–1.0 Hz (see figure 5(*a*)) as a measure of the noise intensity. In spite of this change, the linear dependence on V^2 is verified (see figure 5(*b*)) and so we conclude that equilibrium resistance fluctuations are also in this case the origin of the excess noise.

The results of all our noise measurements are collected in table 2 as the values of dimensionless quantity $S \equiv \langle fS_V \rangle / V^2$, which is frequency and voltage independent. The reasons for which in case of thick-film resistors we should use S rather than commonly used Hooge's parameter α are explained in [15]. Following e.g. [16], we call S (relative) noise index in spite of small differences between the two definitions. Peled *et al* [16] has defined S by the equation

$$S_V = \frac{S}{f^\gamma} V^2, \qquad (1)$$

which means that their S is simply the noise power density at 1 Hz normalized by the square of voltage V. Unlike this 'point' quantity our S is a 'wide-band' measure of normalized noise power density. As for $\gamma = 1$, which is the case for our samples (see table 3), both definitions give almost the same value of S we use this term throughout the rest of this paper. Note that S is a reasonable quantity only when $S_V \sim V^2$ relation holds. At this point thick film resistors differ from other metal–insulator composites, for which noise has been found to vary sublinearly with V^2 [17].

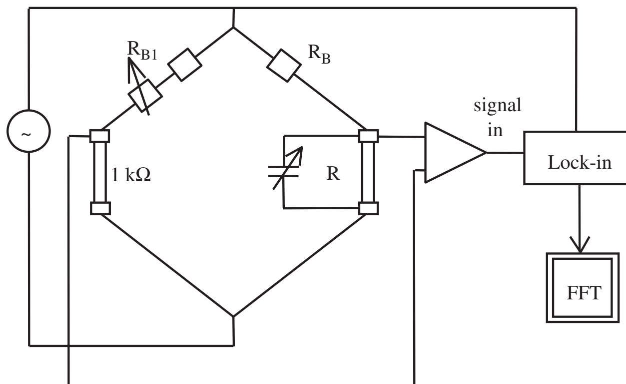

Figure 3. Set-up for AC noise measurements. R_{B1}, R_B and 1 kΩ are wire-wound resistors. R is the resistor under test.

One may wonder why our specimens are chosen to be of different size: we have resistors as small as 0.3×0.3 mm^2 and as large as 9×1 mm^2. The real reason for involving such different samples was to study the volume dependence of the noise index. For example, for the large sample L2041SP-R1, shown in figure 2, we have obtained $S = 7.3 \times 10^{-15}$. At the same time for a small sample L2041SP-R4 measurements gave $S = 1.64 \times 10^{-13}$ (see table 2). The ratio of these two equals 22.46, which is approximately inverse the ratio of the sample volumes $0.3^2/1.5^2 = 1/25$ (if we assume the same average thickness of both resistors). This suggests that noise index S scales as reciprocal volume Ω^{-1} whereas a small difference

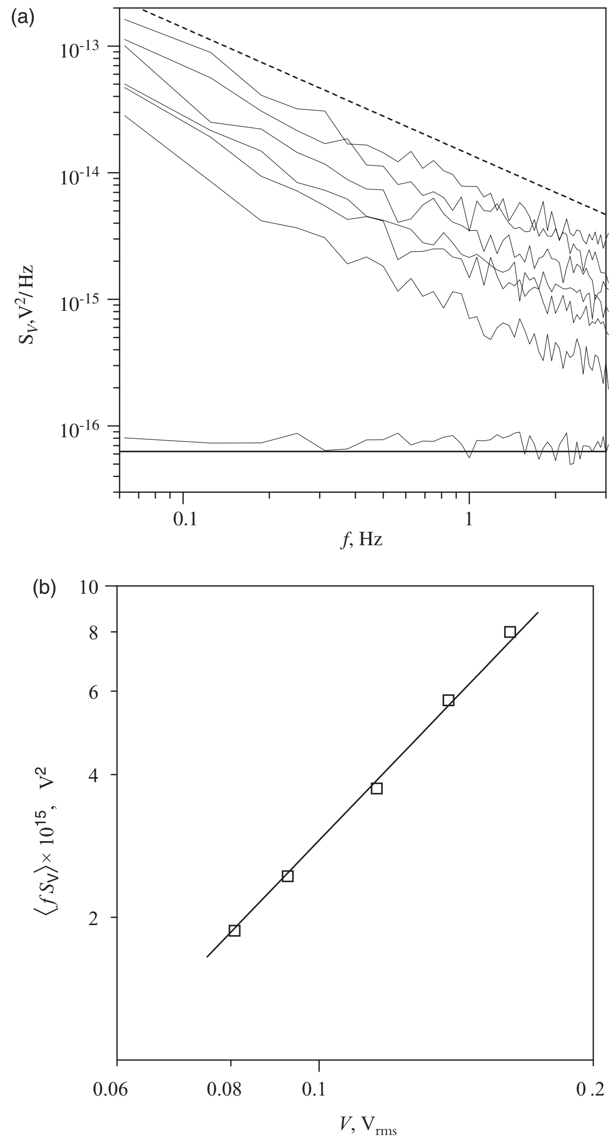

Figure 4. (*a*) Power spectral densities 'as-measured' by AC method for sample L041SC-R4. Note that the noise background, $S_{V=0}$, (the lowest curve) has flat spectrum for $f \to 0$ and equals approximately (——) twice the value of the thermal noise $2 \times \{4kT(R + 1\,\text{k}\Omega)\}+$ preamplifier noise (1.3×10^{-17} V^2 Hz^{-1}). Successive spectra are for $V = 0.069, 0.081, 0.092, 0.115, 0.138, 0.161$ V_{rms}. They scale like V^2 as shown in (*b*) where the line has the slope of 2. Dashed line in (*a*) shows the exact $1/f$ spectrum.

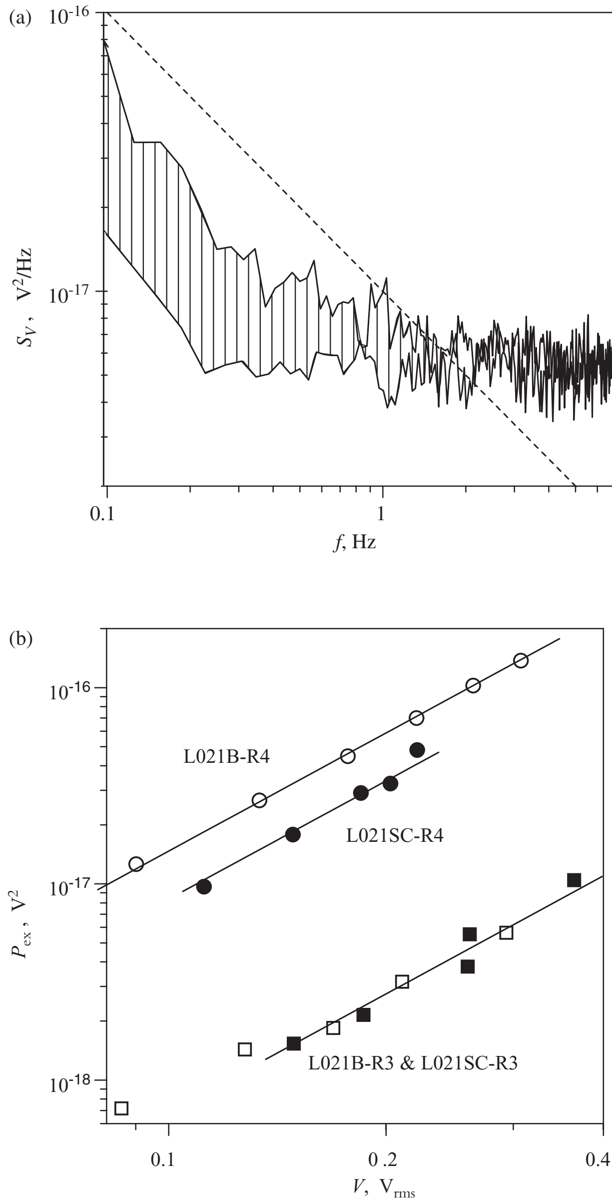

Figure 5. (*a*) Noise spectral densities measured for the sample L021SC-R4 for voltages $V = 0.11\ \mathrm{V_{rms}}$ (upper curve) and $V = 0$ (lower curve). Hatched area is the power P_{ex} of excess noise in the bandwidth 0.1–1 Hz, $P_{ex} = \int_{f_L}^{f_H} (S_V - S_{V=0})\,\mathrm{d}f$. Dashed line shows exact $1/f$ spectrum. In (*b*) P_{ex} is plotted versus voltage V applied to the sample. The lines have the slope of 2 which means that the relation $P_{ex} \sim V^2$ holds. Noise index is calculated as $S = (P_{ex}/\ln 10)/V^2$.

between 22.46 and 25 is due to ordinary sample-to-sample variations (possible reasons for sample-to-sample variations of noise intensity have been discussed, e.g. [18]). Indeed, similar calculations done for other series confirm this scaling (see figures 7 and 8 and text after figure 7). Two substantial conclusions can be derived from $S \sim \Omega^{-1}$ dependence. The first is that resistance fluctuations observed at the sample's tab terminals are the superposition of spatially uncorrelated local resistance fluctuations [19]. The second is that a good measure of the noise properties of the material from which the resistor is fabricated is the product $C \equiv \Omega S$, which is frequency, voltage

Table 2. Noise index $S \equiv \langle f S_V \rangle / V^2$ (in units of 10^{-15}) of the resistors from table 1. For CF021 series S was calculated as described in figure 5 caption.

Specimen	R1	R2	R3	R4	R5
A8039/200	24.2	—	—	372	—
A8039/400	50.7	—	—	438	—
L8039SP	24.4	—	—	537	—
L8039SC	20.6	—	—	257	—
L8039B	40.6	—	—	689	—
A2041/200	8.32	—	—	214	—
L2041SP	7.30	—	—	164	—
L2041SC	4.80	—	—	158	—
L2041B	7.64	—	—	471	—
L2051SC	—	35.0	—	—	3.23
L2051B	—	41.7	—	—	2.60
L2051SC(F)	—	—	—	—	3.81
L2051B(F)	—	—	—	—	7.54
L2051B(H)	—	49.2	—	—	—
L041SC	—	—	159.4	581.3	—
L041B	—	—	171.3	1298	—
L021SC	—	—	0.137	1.675	—
L021B	—	—	0.137	2.939	—

and volume independent (see, e.g. [20, 21]). We will use this measure in section 5 where the noise properties of conventional and various LTCC resistors will be analysed. In the next section we will return to the statistical independence of local resistance fluctuations and provide just other arguments in support of this feature.

4. Second spectral analysis

Consider the power P of noise signal accumulated in some band $f_L \leqslant f \leqslant f_H$, $P = \int_{f_L}^{f_H} S_V(f)\,\mathrm{d}f$. In general P is a function of time and the spectrum of $P(t)$ can be calculated. This power spectrum is called the 'second spectrum' and is denoted by $S^2(F)$. When the physical origin of the noise is a superposition of a large number of statistically independent fluctuators its second spectrum is white at low-frequencies. Such noise is termed Gaussian. In contrast, non-Gaussian noise has been attributed to non-white $S^2(F)$. Deviations from Gaussian behaviour usually arise from a small number of fluctuators and/or correlation between individual fluctuators [22, 23]. Recently Seidler *et al* [24] have shown that when transport is strongly inhomogeneous, non-Gaussian noise is possible even for non-interacting, statistically independent fluctuators. Experimental evidence for this have been reported by Seidler and Solin [25] who found non-Gaussian noise in granular carbon resistor of resistance $R = 1.61\ \mathrm{k}\Omega$. For the sample of dimensions (0.2 mm long $\times$ 1 mm wide $\times$ 1 μm thick) they have found $1/f$ noise with noise index $\langle f S_V \rangle / V^2 \cong 10^{-9}\ \mathrm{Hz}^{-1}$ and large non-white second spectrum. In view of this, it is important to ask what about the non-Gaussian effects in our LTCC resistors. The first reason for this is that transport in thick film resistors is certainly strongly inhomogeneous. The other one is that non-Gaussian noise was found for granular-material resistors of size and resistance comparable to ours. Below we present the results of the measurements of noise Gaussianity of one of our LTCC resistors. We have chosen the sample L8039B-R1 for two reasons. The first reason is that burying is the subject

Table 3. Noise exponent γ of the resistors from tables 1 and 2. Uncertainties in the parenthesis are taken from the spread of γs we have got for different voltages applied to the resistors (no systematic $\gamma(V)$ variation has been observed).

Specimen	R1	R2	R3	R4	R5
A8039/200	1.014 (37)	—	—	1.002 (15)	—
A8039/400	1.033 (15)	—	—	1.066 (50)	—
L8039SP	0.978 (05)	—	—	1.124 (57)	—
L8039SC	1.004 (08)	—	—	1.026 (40)	—
L8039B	0.980 (10)	—	—	0.981 (45)	—
A2041/200	1.084 (59)	—	—	1.035 (11)	—
L2041SP	1.005 (18)	—	—	1.039 (68)	—
L2041SC	1.016 (15)	—	—	1.034 (34)	—
L2041B	0.990 (25)	—	—	0.985 (102)	—
L2051SC	—	1.055 (08)	—	—	1.116 (60)
L2051B	—	0.964 (08)	—	—	1.027 (44)
L2051SC(F)	—	—	—	—	1.071 (24)
L2051B(F)	—	—	—	—	1.012 (22)
L2051B(H)	—	1.007 (34)	—	—	—
L041SC	—	—	1.117 (61)	1.024 (53)	—
L041B	—	—	1.027 (47)	1.090 (50)	—

of this work and we are particularly interested in preserving noise Gaussianity in this process. The second one is that sheet resistance of this sample, 8890 Ω per square lies in the middle of R per square range (100 Ω per square to 100 kΩ per square) examined.

The measurements were performed by DC method. To calculate the second spectra, a series of 27 000 time records each of 2 s duration was digitized and stored. For each time record fast-Fourier transform and power spectral density were calculated. Several tens of bins (FFT points) of each spectrum were then summed up into three bands. The first band ($f_{1\mathrm{L}} = 12$ Hz, $f_{1\mathrm{H}} = 24.5$ Hz) consists of 26 bins, the second one ($f_{2\mathrm{L}} = 25$ Hz, $f_{2\mathrm{H}} = 49$ Hz) consists of 49 bins and the third one ($f_{3\mathrm{L}} = 51$ Hz, $f_{3\mathrm{H}} = 99$ Hz) consists of 97 bins. Time records of powers P_i in each band i, ($i = 1, 2, 3$) are shown in figure 6(a). For each such record the (second) spectrum $S_i^2(f_{i\mathrm{H}}, f_{i\mathrm{L}}, F)$ was calculated. After normalization by the square of average power $\langle P_i \rangle$ it has been displayed in figure 6(b) as $s_i^2 \equiv S_i^2/\langle P_i \rangle^2$. In this figure lines are drawn for Gaussian $1/f$ noise, which was shown to have normalized second spectrum [25],

$$s_i^2 \equiv \frac{S_i^2}{\langle P_i \rangle^2} = \frac{2}{F} \frac{\ln[(f_{i\mathrm{H}} - F)(f_{i\mathrm{L}} + F)/f_{i\mathrm{H}} f_{i\mathrm{L}}]}{[\ln(f_{i\mathrm{H}}/f_{i\mathrm{L}})]^2}. \quad (2)$$

As we can see the spectra follow exactly the theoretical lines, which proves that noise in L8039B-R1 sample is Gaussian. This is in line with the conclusion derived in the previous section from the volume dependence of noise index.

5. Noise versus substrate, firing and burying

The main conclusions of this paper come from the analysis of volume independent noise intensity C. Its values calculated for majority of our resistors are displayed in figures 7 and 8. Before we proceed further we should emphasize that when calculating the resistors' volumes we have assumed their uniform thickness, $d = 10\,\mu$m. For buried resistors we have also assumed that their surface is reduced by 24% due to the tape shrinkage during firing.

The first conclusion we can draw from the data is that indeed, C is volume independent and as such it measures well noise properties of the material of which the resistor is fabricated. For DP2041 and DP8039 series, for which large (R1) and small (R4) samples differ in volume by 25 times, we get the values of C that differ no more than 3 times (see figure 7). For other series, for which the difference in volume of large and small resistors is smaller (16 for CF041 and CF021 series and 9 for DP2051 series), the difference in values of C is even smaller than in the previous case (see figure 8). This spread of C is small, of the order of usually observed for specimens of the same size, and can be interpreted as arising from sample-to-sample variations [18].

The second conclusion can be drawn for the series DP2041 and DP8039, for which the most complete set of data has been collected. For these series noise intensities of LTCC resistors are of the same order as of resistors on alumina substrates. We conclude that LTCC tape and resistive ink form a well-matching system. The interactions between them which take place during (co)firing do not change noise properties of the resistive material itself. This is confirmed also by the data for DP2051 series. Here the resistors were printed on various LTCC tapes but in all cases the noise intensities C fall into relatively narrow range (2–5) $\times$ 10^{-25} m^{-3} (see figure 8).

Eventually, the third conclusion that can be drawn from our experiment is that burying leads to increase of sheet resistance, but not (or very little) of noise intensity C (see figure 8). The most pronouncing example is the resistor R4 of DP2041 series. Here more than 10 times increase of R per square is associated with merely twice increase of C. In the following we will comment on this surprising behaviour.

First of all let us note that the naive explanation of the above effect is that the change of sheet resistance, observed in the process of burying, is due to the simple geometrical effect. Namely, R per square increases because the film is getting thinner during burying. This must be rejected, since to have an order of magnitude of rising up the resistance, as we have for DP2041 series, the surface area of the sample should be several times greater for the volume to be conserved. This is certainly not the case since the outline of the buried resistor is still visible when has been put against the light, and it does not change when burying. On the other hand, our resistors are only 10 μm thick, so that interface layers between LTCC

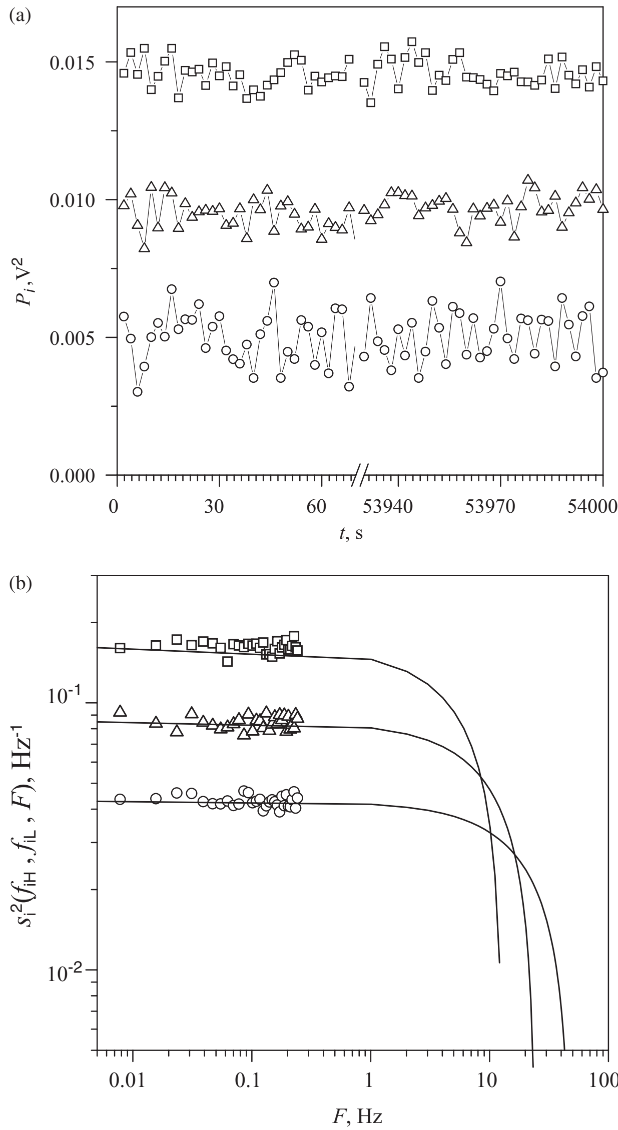

Figure 6. (a) Noise power P_i in the band i ($i = 1, 2, 3$) as a function of time for L8039B-R1 resistor biased by the DC voltage $V = 13.157$ V. The curves have been offset by 0.005 (P_2) and 0.01 (P_1) for clarity. (b) Normalized second spectra calculated for the signals from (a): (□) band 12–24.5 Hz, (△) band 25–49 H (○) band 51–99 Hz. Lines are drawn according to equation (2).

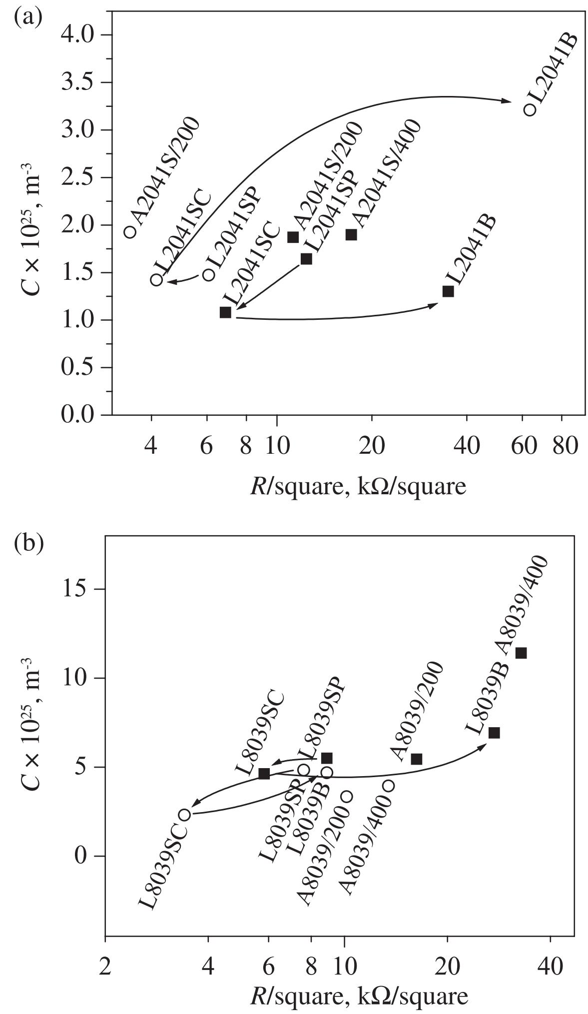

Figure 7. Noise intensity $C \equiv S\Omega$ calculated for the resistors from DP2041 series (a) and from DP8039 series (b) versus sheet resistance R per square. Open symbols refer to small samples R4. Filled symbols are for large samples R1.

and resistive material contribute significantly to the overall resistance [2]. In this case the change of resistor thickness d could lead to change of resistance, which is not linear with d. Even a small change of d could lead to a large change of sheet resistance. In principle, such change of resistance is caused by the change of effective resistivity ρ and would be associated with no change of noise intensity, provided C depends on ρ weakly. Thus, we come to the conclusion that, during burying resistance increases due to increase of effective resistivity and this increase is not associated with simultaneous increase of noise intensity. Usually those two are somehow correlated and simultaneous increase of both ρ and C is observed. For example, if burying led to the increase of grains sizes but not to the increase of microscopic grain-to-grain resistances and noise intensities, the relation $C \sim \rho^3$ would be observed [26].

If the resistance increase was due to the increasing tortuousity of the percolation path, we would expect the relation $C \sim \rho^w$ with exponent $w \cong 0.8$ for classical percolation [27] or $w \cong 2.1$ or 2.4 for continuum percolation [28] or $w \cong 3$ for the case when small currents flow also through non-ideal 'noisy' insulator surrounding the (existing!) percolation cluster [27, 29–31]. Another possibility is the change of resistivity due to the increase of microscopic grain-to-grain resistance r. Here the increase of r would be associated with the significant increase of C, provided a microscopic charge transport mechanism is of metallic origin. Namely, $C \sim r^3$ is expected for diffusive (Maxwell) contact [32] or $C \sim r^{3/2}$ for ballistic (Sharvin) contact [33]. Also for the Ohmic conduction through a thin glassy layer between adjacent conductive oxide grains the relation $C \sim r^1$ is expected [33]. Eventually, we come to the case of grain-to-grain tunnelling. This case calls for special attention because recent studies of LTCC resistors microstructure show that burying leads to grain coarsening, increase of grain-to-grain separations and thus the (significant) increase of r [2]. In the next section we shall discuss this conduction mechanism in more details.

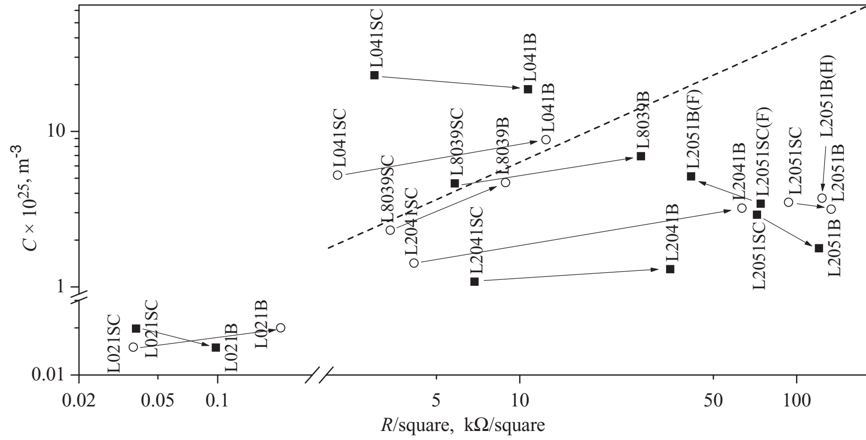

Figure 8. Noise intensity C versus sheet resistance R per square for surface co-fired (SC) and buried (B) LTCC resistors from table 1. Arrows pin up the samples from the same series and point to the buried ones. Dotted line has the slope of 0.8 and shows the weakest C versus R per square dependence in case when microscopic conduction mechanism is other than tunnelling. Open and filled symbols are for 'small' and 'large' samples, respectively.

6. Tunnelling conduction

Although there is no unique theory of low-frequency noise in the tunnelling like transitions it is possible to write down the relation between noise intensity C_t and resistance r_t of a single tunnelling junction in the form [34]

$$C_t \sim r_t^{\theta} \qquad (3)$$

provided all weaker than exponential dependencies of C_t on junction thickness are neglected. The most likely value of exponent θ is $\theta = 0$, although values different from 0 are also possible. Celasco *et al* [35] (also Rogers and Buhrman [36]) have shown that fluctuations of charge in impurity states in the barrier insulator lead (via the barrier height fluctuations) to the fluctuations δg_t of tunnelling conductance $g_t = 1/r_t$. From their results

$$\{\delta g_t^2\} \sim A_1 \left(4\pi\sqrt{\frac{2mE_b}{h^2}}s - 1\right)^2 g_t^2, \qquad (4)$$

where the braces denote time averaging, m is electron effective mass, h is Planck's constant, E_b and s are the mean barrier height and width, respectively, and A_1 contains a reciprocal dependence on the junction area, it stems that $\theta = 0$. Kogan and Nagaev [37] have assumed that a mobile atom or group of atoms in disordered barrier insulator turn on or off one of the tunnelling channels and thus the magnitude of δg_t is of the order of g_t/N_t, where N_t is the number of tunnelling channels. We have $\{\delta g_t^2\} \sim g_t^2$, and, $\theta = 0$ again. However, when the fluctuating atom (ion) switches the channel between direct and resonant tunnelling, then the magnitude of δg_t is of the order of $g_t^{1/2}$ [38]. In this case $\{\delta g_t^2\} \sim g_t$, $C_t \sim \{\delta g_t^2\}/g_t^2 \sim r_t$ and $\theta = 1$ rather than 0.

Coming back to our LTCC resistors, let us note that with exponent $\theta = 0$ equation (3) explains the weak C versus ρ dependence, provided this microscopic relation is preserved when noise and resistance are measured across the macroscopic device (resistor). This is not a trivial question, since grain-to-grain separations are not the same for all junctions in the resistor but are rather randomly distributed. As g_t depends on s exponentially, we have to consider the network of microscopic resistances distributed widely on logarithmic scale [39]. The adoption of the critical path analysis [40] has allowed the authors of [41] to show that, indeed, macroscopic noise intensity preserves microscopic relation of equation (3) exact to the logarithmic term

$$C \sim (\ln \rho)^{\nu(3-\theta)} \rho^{\theta}, \qquad (5)$$

where $\nu = 0.89$ the percolation correlation length exponent in three dimensions [42]. Equations (3) and (5) with very probable value of exponent $\theta = 0$ are able to explain our experiment at least qualitatively: grains coarsening that takes place during burying leads to a small increase of grain-to-grain separations. This rises up microscopic resistances but not the noise intensities. On the resistor tabs these changes are observed as the increase of sheet resistance and much weaker increase of noise intensity. One more argument can be adduced in support of this picture. Theoretical result of equation (5) is quite general and should hold also for the case when the change of resistance is caused by the reasons other than burying. For example, by the change of metal content of a metal–insulator composite. In the region below the percolation threshold, tunnelling junctions between metallic clusters take part in the conduction process. We expect that as the metal volume fraction decreases, ρ increases due to the increasing number of tunnelling junctions in the percolation path. At the same time, only very weak increase of noise intensity C is expected, if $\theta = 0$ in equation (5). Experiments confirm this scenario. A plateau in C versus ρ for large ρs has been observed for Pt/Al_2O_3 granular metals [20], carbon black/polymer composites [43] and RuO_2/glass 'on alumina' thick film resistors [44, 45]!

7. Conclusions

In the summary we would like to conclude that noise measurements performed with DC or AC techniques show that low-frequency $1/f$ noise observed in LTCC resistors is a purely Gaussian process resulting from a superposition of

independent microscopic fluctuators. This was concluded from the volume dependence of noise index as well as from direct measurement of the second spectra. Comparison of the volume independent noise intensities of conventional resistors on alumina substrates and LTCC resistors shows that, on average, noise properties of LTCC resistors are not worse than those of conventional thick-film resistors. This is important from the 'practical' point of view. Eventually, a detailed study of co-fired surface resistors and buried resistors shows that burying a resistor in a LTCC surrounding usually leads to (significant) increase of resistance, while the noise intensity is kept on the same level. We interpret it as a fingerprint of tunnelling as the dominant conduction mechanism in LTCC resistors. This is in line with current understanding of charge transport in thick-film resistors. Moreover, recently it was shown that tunnelling barrier model of Pike and Seager [46], which dealt with the classical thick-film resistors, can be successfully applied to the explanation of electrical properties of LTCC resistors [6]. As shown by Chen *et al* [47] this model is able to explain $1/f$ noise in classical thick-film resistors. In view of our results this statement can probably be extended also to LTCC resistors.

Acknowledgments

This work was supported by the Polish Committee for Scientific Research, Grant no 8T11B 055 19. The authors are gratefully indebted to I Talle and R Sikora for their critical readings of the manuscript.

References

[1] Sutterlin R C, Dayton G O and Biggers J V 1995 *IEEE Trans. Comp., Packg. Manuf. Technol.—Part B* **18** 346
[2] Rodriguez M, Yang P, Kotula P and Dimos D 2000 *J. Electroceramics* **5** 217
[3] Ting C-J, His C-S and Lu H-Y 2000 *J. Am. Ceram. Soc.* **38** 2945
[4] Dziedzic A, Golonka L, Kita J, Thust H, Drue K-H, Bauer R, Rebenklau L and Wolter K-J 2001 *Microelectronics Reliab.* **41** 669
[5] Fu S L and Hsi C-S 2001 *Proc. 2001 Int. Symp. Microelectronics (IMAPS-US) (Baltimore)* ed B Romeshko, p 190
[6] Yang P, Rodriguez M, Kotula P, Miera B K and Dimos D 2001 *J. Appl. Phys.* **89** 4175
[7] Delaney K, Barrett J, Barton J and Doyle R 1999 *IEEE Trans. Adv. Packg.* **22** 78
[8] Dziedzic A, Drue K-H, Kita J, Kolek A and Ptak P 2002 *Proc. 26th IMAPS-Poland Conf. (Warsaw)* p 61
[9] Wang G, Barlow F D and Elshabini A 2002 *Proc. 2002 Int. Symp. on Microelectronics (Washington: IMAPS) (Denver)* ed R Charbonneau and S Tek, p 851
[10] Dziedzic A, Golonka L, Kolek A, Mach P and Nitsch K 2001 *Proc. 24th Int. Spring Seminar on Electronics Technology, ISSE'2001 Calimanesti-Caciulata (Romania)* ed I Dumitrache and P Svasta, p 137
[11] Ptak P, Kolek A and Dziedzic A 2002 *Proc. 25th Int. Spring Seminar on Electronics Technology, ISSE'2002 (Prague)* ed P Mach and J Urbanek (Czech Republic: Czech Technical University) p 142
[12] Dziedzic A, Golonka L, Kita J and Mielcarek W 2002 *Proc. 25th Int. Spring Seminar on Electronics Technology, ISSE'2002 (Prague)* ed P Mach and J Urbanek (Czech Republic: Czech Technical University) p 133
[13] Scofield J H 1987 *Rev. Sci. Instrum.* **58** 985
[14] Koch R H 1993 *Phys. Rev.* B **48** 12217
[15] Vandamme L K J and Trefan Gy 2002 *IEE Proc.-Circuits Devices Syst.* **149** 3
[16] Peled A, Johanson R E, Zloof Y and Kasap S O 1997 *IEEE Trans. Comp., Packg. Manuf. Technol.—Part A* **20** 355
[17] Nandi U N, Mukherjee C D and Bardhan K K 1996 *Phys. Rev.* B **54** 12903
[18] Masoero A, Morten B, Tamborin M and Prudenziati M 1995 *Microelectron. Int.* **37** 5
[19] Butterweck H 1975 *Philips Res. Rep.* **30** 316
[20] Mantese J V and Webb W W 1985 *Phys. Rev. Lett.* **55** 2212
Mantese J V, Curtin W A and Webb W W 1986 *Phys. Rev.* B **33** 7897
[21] Dziedzic A and Kolek A 1998 *J. Phys. D: Appl. Phys.* **31** 2091
[22] Restle P J, Hamilton R J, Weissman M B and Love M S 1985 *Phys. Rev.* B **31** 2254
[23] Parman C E, Israeloff N E and Kakalios J 1993 *Phys. Rev.* B **47** 1097
[24] Seidler G T, Solin S A and Marley A C 1996 *Phys. Rev. Lett.* **76** 3049
[25] Seidler G T and Solin S A 1996 *Phys. Rev.* B **53** 9753
[26] Wolf M, Muller F and Hemschik H 1985 *Active and Passive Elec. Comp.* **12** 59
[27] Tremblay A M S, Fourcade B and Breton P 1989 *Physica* A **157** 89
[28] Tremblay A M S, Feng S and Breton P 1986 *Phys. Rev.* B **33** 2077
[29] Morozovsky A E and Snarskii A A 1989 *Sov. Phys. JETP* **68** 1066
[30] Tremblay R R, Albinet G and Tremblay A M S 1991 *Phys. Rev.* B **43** 11547,
Tremblay R R, Albinet G and Tremblay A M S 1992 *Phys. Rev.* B **45** 775
[31] Kolek A 1992 *Phys. Rev.* B **45** 205
[32] Vandamme L K J 1987 *IEEE Trans. Comp. Hybrid Manuf. Technol. CHMT* **10** 290
[33] Pierre C, Deltour R, Van Bentum J, Perenboom J A and Rammal R 1990 *Phys. Rev.* B **42** 3386
[34] Snarskii A A and Kolek A 1996 *Sov. Phys. JETP Lett.* **63** 651
[35] Celasco M, Masoero A, Mazzetti P and Stepanescu A 1978 *Phys. Rev.* B **17** 2553
Celasco M, Masoero A, Mazzetti P and Stepanescu A 1978 *Phys. Rev.* B **17** 2564
[36] Rogers C T and Buhrman R A 1983 *IEEE Trans. Magnetics* **19** 453
[37] Kogan Sh M and Nagaev K E 1984 *Pis'ma Zh. Eksp. Teor. Fiz.* **10** 313
[38] Speakman A M and Adkins C J 1992 *J. Phys.: Condens. Matter* **4** 8053
[39] Tyć S and Halperin B I 1989 *Phys. Rev.* B **39** 877
[40] Ambegaokar V, Halperin B I and Langer J S 1971 *Phys. Rev.* B **4** 2612
[41] Morozovsky A E and Snarskii A A 1993 *Sov. Phys. JETP* **77** 959
[42] Stauffer D and Aharony A 1994 *Introduction to Percolation Theory* (London: Taylor and Francis)
[43] Breeze A J, Carter S A, Alers G B and Heaney M B 2000 *Appl. Phys. Lett.* **76** 592
[44] Bobran K and Kusy A 1991 *J. Phys.: Condens. Matter* **3** 7015
[45] Bobran K 1989 *Z. Phys.* B **75** 507
[46] Pike G E and Seager C H 1977 *J. Appl. Phys.* **48** 5152
[47] Chen T M, Su S F and Smith D 1982 *Solid State Electron.* **25** 821